BMC Biology

RESEARCH

Open Access

Expression of a pheromone binding protein affected by timeless gene governs female mating behavior in *Bactrocera dorsalis*

Yuting Jiao[1†], Guohong Luo[1†], Yongyue Lu[1] and Daifeng Cheng[1*]

Abstract

Background The rhythmic mating behavior of insects has been extensively documented, yet the regulation of this behavior through sex pheromone sensing olfactory genes affected by the clock genes in the rhythm pathway remains unclear.

Results In this study, we investigated the impact of circadian rhythm on female recognition of male rectal *Bacillus*-produced sex pheromone in *B. dorsolis*. Behavioral and electrophysiological assays revealed a peak in both mating behavior and response to sex pheromones in the evening in females. Comparative transcriptome analysis of female heads demonstrated rhythmic expression of the Timeless gene-Tim and odorant binding protein gene-Pbp5, with the highest expression levels occurring in the evening. Protein structural modeling, tissue expression patterns, RNAi treatment, and physiological/behavioral studies supported Pbp5 as a sex pheromone binding protein whose expression is affected by Tim. Furthermore, manipulation of the female circadian rhythm resulted in increased morning mating activity, accompanied by consistent peak expression of Tim and Pbp5 during this time period. These findings provide evidence that insect mating behavior can be modulated by clock genes through their effects on sex pheromone sensing processes.

Conclusions Our results also contribute to a better understanding of the molecular mechanisms underlying rhythmic insect mating behavior.

Keywords *Bactrocera dorsalis*, Sex pheromone, Pheromone binding protein, Timeless gene

Background

Reproductive behavior, including courtship, mating, and oviposition, is a fundamental biological activity for insects to regulate their populations [1]. Mating behavior serves as the pivotal step in reproductive activity [2] and is typically initiated following successful courtship [3]. During courtship, sexually mature individuals utilize pheromones, visual signals, or vocalizations to attract potential mates from a distance [4–6]. At close range, they employ visual, olfactory, and tactile cues to express affection and facilitate acceptance of mating behavior from the opposite sex [7].

Environmental factors exert a significant influence on the mating behavior of insects [8]. The periodic fluctuations in light serve as crucial signaling cues that impact the courtship and mating behavior of most insects [7, 9]. Environmental changes in light, coupled with temperature variations, represent important entrainment factors affecting insect mating behavior [10]. The circadian rhythm is an endogenous biological process driven by molecular oscillations of the internal clock [11].

†Yuting Jiao and Guohong Luo contributed equally to the study.

*Correspondence:
Daifeng Cheng
chengdaifeng@scau.edu.cn
[1] Department of Entomology, South China Agricultural University, Guangzhou 510640, China

Most central clocks undergo endogenous cyclic oscillations within the central nervous system of organisms [12–14]. Peripheral clocks, under the influence of the central clock, modulate various behaviors in organisms [15, 16]. Extensive research has been conducted on the role of the peripheral nervous system in animal pheromone-mediated courtship behaviors [17–19]. Circadian rhythms governing mating behavior play a pivotal role in population survival and propagation among animals [20]. Mating behavior that occurs at a specific time enables animals to evade adverse environmental conditions such as predators and concentrate reproductive activities at opportune times based on their ecological niches, thereby enhancing safe reproduction and promoting stable population growth [21]. A comprehensive understanding of how and why animals mate at specific times provides valuable insights into their reproductive strategies, evolutionary adaptations, and ecological interactions, offering guidance for conservation efforts, wildlife management strategies, and agricultural pest control initiatives.

Previous research has suggested that male *B. dorsalis* release rectal *Bacillus* produced pyrazine compounds (trimethylpyrazine (TMP) and tetramethylpyrazine (TTMP)) as sex pheromones in the evening to attract females for mating [22, 23]. However, it remains unclear how females perceive the pheromone signal and whether their response is limited to the evening. In this study, we further demonstrate that female mating behavior exhibits rhythmicity, occurring exclusively in the evening. Electroantennogram (EAG) recordings and behavioral assays indicate a rhythmic variation in female sensitivity to sex pheromones, peaking in the evening. Comparative head transcriptome analysis reveals that the sex pheromone binding protein-Pbp5 is responsible for binding the sex pheromone. Furthermore, we show that the clock gene-Timeless (Tim) can regulate the rhythmic expression of Pbp5. This study contributes to our understanding of insect reproductive behavior and serves as an important supplement to research on insect olfactory perception.

Results

Mating behavior of females and their attraction to sex pheromone peaking in the evening

To investigate whether female mating occurs at specific times of the day, we monitored mating frequency throughout the day. The results revealed that females only mate in the evening, particularly at 20:00 (Fig. 1a). Previous research has demonstrated that TMP and TTMP are male-derived sex pheromone that effectively attracts females [22–24]. We hypothesized that differences in female sensitivity to TMP and TTMP may account for variations in mating frequency at different times of day. To test this hypothesis, we assessed the attractiveness of TMP and TTMP to females at various time points throughout the day. Our findings indicated that TMP and TTMP strongly attracted females only in the evening, especially at 20:00 (Fig. 1b), consistent with the observation on mating frequency. Furthermore, EAG recordings showed that both TMP and TTMP elicited stronger responses from female antennae in the evening compared to the morning (Fig. 1c–h). These results suggest that both mating behavior and response to sex pheromone peak in the evening.

Screening for genes associated with rhythmic mating behavior

To further screen and identify the olfactory and clock genes that regulate the rhythmic mating of females, we conducted female head RNA-seq analysis at 4-h intervals throughout the day. The results revealed no significant differences in head gene expression patterns at different times of the day (Additional file 1: Fig. S1a, Additional file 2: Dataset S1). However, the comparison of female head samples collected at different times led to a greater number of identified differentially expressed genes (DEGs) (Fig. 2a, Additional file 1: Fig. S1b–1f and Additional file 3–7: Datasets S2–S6). Subsequently, KEGG analysis was performed on most DEGs screened between 8:00 and 20:00 to identify genes responsible for regulating rhythmic mating behavior in females. The results revealed a significant enrichment of the circadian rhythm pathway (Fig. 2b). Analysis of gene expression patterns for differentially expressed genes (DEGs) in the circadian rhythm pathway indicated high expression of Tim in the heads of females at 20:00 (Fig. 2c and e, Additional file 8: Dataset S7). Given that olfactory genes, such as chemosensory proteins (Csps), odorant binding proteins (Obps), and odorant receptors (Ors), are primarily responsible for binding volatiles, including sex pheromones [25], we analyzed the expression patterns of olfactory genes in female heads at different times to identify potential genes involved in sex pheromone binding. The results showed differential expression of various olfactory genes between heads at 8:00 and 20:00 (Fig. 2d, Additional file 9: Dataset S8). Among these genes, pheromone binding protein 5 (Pbp5) exhibited the highest and lowest expressions at 20:00 and 8:00, respectively, suggesting its role in sex pheromone binding. To further investigate Pbp5 function, odorant binding protein 99a (Obp99a), which displayed high expression across all sampling times, was selected as the control gene for subsequent functional analysis. qPCR results also demonstrated high expression of Pbp5 in female antennae at 20:00 (Fig. 2f). These findings suggest that peak mating behavior among

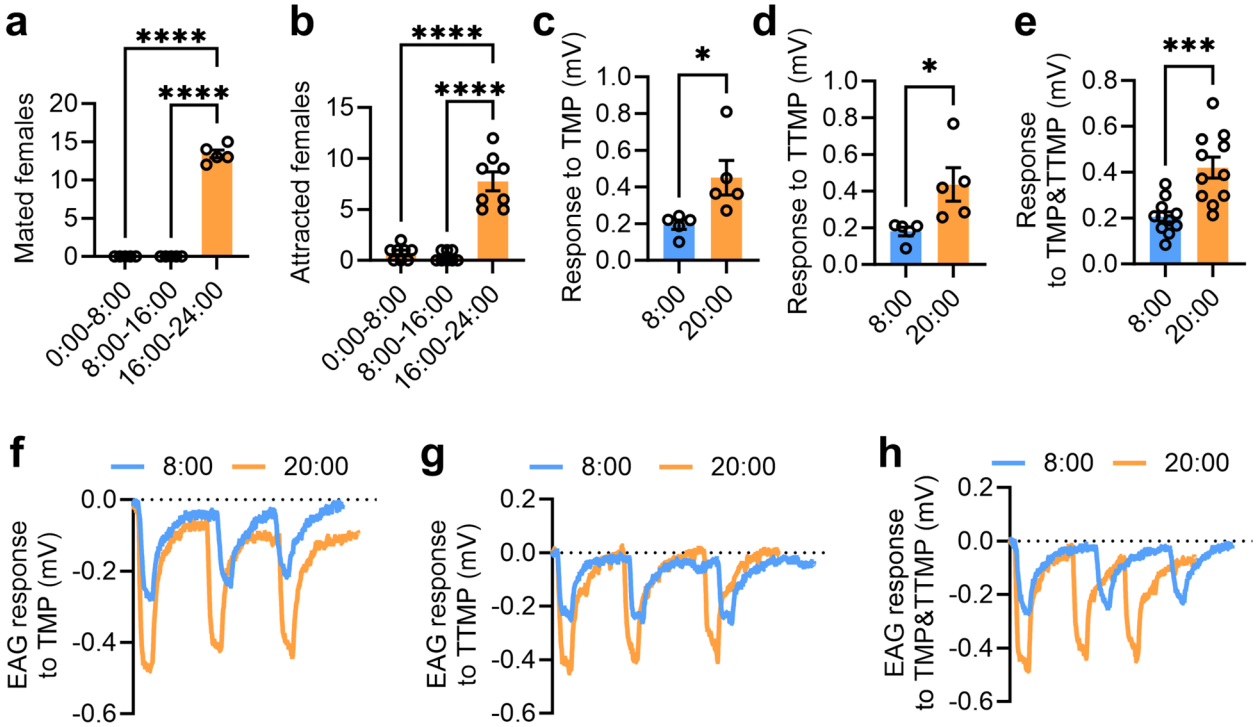

Fig. 1 Female mating behavior and attraction to sex pheromone peak in the evening. **a** Number of mated females at different time periods in a day (replicates = 5, $F(2,12) = 690.6$, $P < 0.0001$, one-way ANOVA). **b** Number of females attracted by sex pheromone at different time periods in a day (replicates = 8, $F(2,21) = 54.83$, $P < 0.0001$, one-way ANOVA). **c** Female EAG response to TMP at 8:00 and 20:00 (replicates = 5, $P = 0.0295$, independent sample *t* test). **d** Female EAG response to TTMP at 8:00 and 20:00 (replicates = 5, $P = 0.0259$, independent sample *t* test). **e** Female EAG response to TMP and TTMP mixture at 8:00 and 20:00 (replicates = 11, $P = 0.0004$, independent sample *t* test). **f** Example traces of female antenna responses to TMP. **g** Example traces of female antenna responses to TTMP. **h** Example traces of female antenna responses to mixture of TMP and TTMP

females at 20:00 may be associated with elevated levels of Tim and Pbp5.

Pbp5 exhibits robust binding capabilities to both TMP and TTMP

The interaction between Pbp5 and the ligands (*N*-phenyl-1-naphthylamine (1-NPN), TMP, and TTMP) was predicted using Alphafold 2.0 for homology modeling of Pbp5, followed by prediction of the interaction sites with Autodock Vina (Additional file 1: Fig. S2a). The evaluation results indicated a high-quality score of 96.7 for the constructed Pbp5 model (Additional file 1: Fig. S2b), and all amino acids fell within the optimal and suboptimal regions in the Ramachandran Plot (Additional file 1: Fig. S2c), suggesting suitability for docking analysis. The docking results revealed that Phe-31, Ile-52, Lys-55, Phe-95, and Phe-147 constituted the binding site of Pbp5 to 1-NPN (Fig. 3a, Additional file 10: Table S1). Additionally, Ile-28, Phe-31, Phe-95, and Phe-147 were identified as the binding sites of Pbp5 to TMP and TTMP (Fig. 3b and c, Additional file 10: Table S1). Furthermore, it was found that Phe-31, Phe-95, and Phe-147 were common binding sites for TMP, TTMP, and 1-NPN to Pbp5 (Additional file 10: Table S1), suggesting that competitive fluorescence binding experiments between TMP (TTMP) and 1-NPN could be conducted to assess the binding affinity of TMP (TTMP) to Pbp5. Subsequent ligand binding assays demonstrated strong interaction between 1-NPN with recombinant Pbp5 protein with a dissociation constant (Kd) of 10.57 μM (Fig. 3d). Moreover, competitive fluorescence binding experiments indicated that both TMP and TTMP exhibited stronger affinities towards Pbp5 compared to 1-NPN with the inhibition constant (Ki) of 0.2243 μM and 0.2101 μM, respectively (Fig. 3e and f). Then the recombinant protein of Pbp5 with the predicted binding sites to TMP and TTMP being mutated (Ile-28, Phe-31, Phe-95, and Phe-147 mutated to Ala) were expressed and purified. Subsequent ligand binding assays showed 1-NPN still had strong binding ability to the mutant Pbp5 protein with a Kd value of 33.89 μM (Fig. 3g). However, competitive fluorescence binding experiments indicated that both TMP and TTMP exhibited almost no affinities towards mutant Pbp5 protein with Ki values of 3e + 31 μM and 9e + 24 μM, respectively (Fig. 3h and i). These findings suggest that

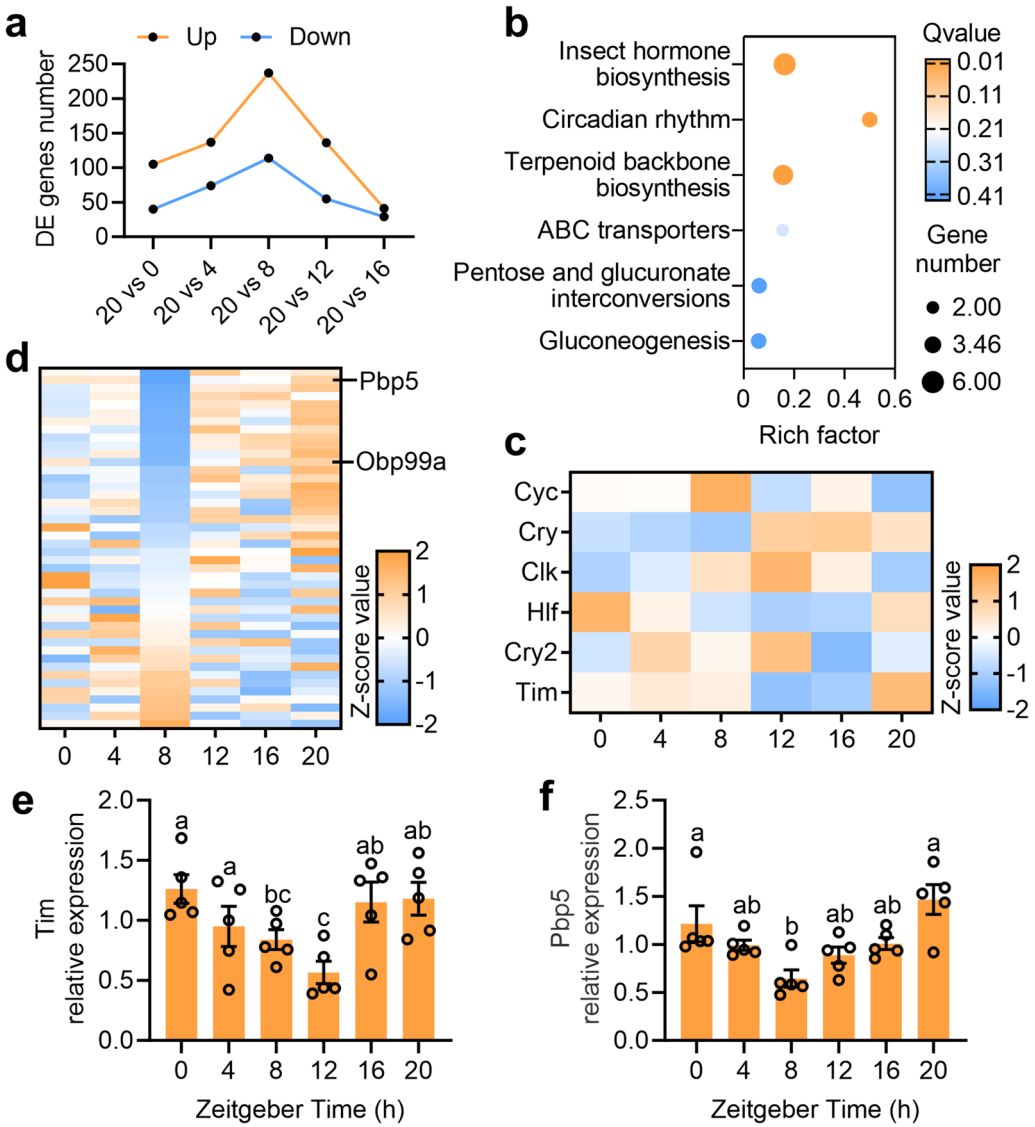

Fig. 2 Tim and Pbp5 screened by transcriptome analysis may be associated with peaking mating behavior of females at 20:00 in a day. **a** The number of DEGs in the female head at 20:00 compared with those at other times. Up: significantly up expressed genes in the head of females at 20:00; down: significantly down expressed genes in the head of females at 20:00. **b** KEGG pathways enriched with the DEGs between female heads at 20:00 and 8:00. **c** Expression patterns of DEGs (between 20:00 and 8:00) in the circadian rhythm pathway at different times in a day. Before heat mapping, the FPKM values of the DEGs were processed using *Z*-score standardization. (d) Expression patterns of the olfactory genes in the head of females at different times in a day. Before heat mapping, the FPKM values were processed using *Z*-score standardization. **e** Relative expression verification of Tim in the head of females at different times in a day (replicates = 5, $F(5,24) = 3.906$, $P = 0.0099$, one-way ANOVA). **f** Relative expression verification of Pbp5 in the head of females at different times in a day (replicates = 5, $F(2,24) = 5.866$, $P = 0.0011$, one-way ANOVA)

TMP and TTMP can effectively bind to Pbp5 and may regulate the rhythmic mating behavior of females.

RNAi-mediated knockdown of Pbp5 results in impaired female mating and reduced EAG response to TMP and TTMP

We then conducted an investigation into the role of Pbp5 through sequence similarity analysis and RNAi. A maximum likelihood phylogenetic analysis using amino acid sequence alignments for 10 Obps from various Diptera species revealed that Pbp5 was highly conserved within Tephritidae (Fig. 4a). The majority of amino acids were conserved within the selected species, particularly the four signature cysteine residues of Obps (Fig. 4b). Gene expression analysis demonstrated that Pbp5 exhibited the highest expression in female antennae, while

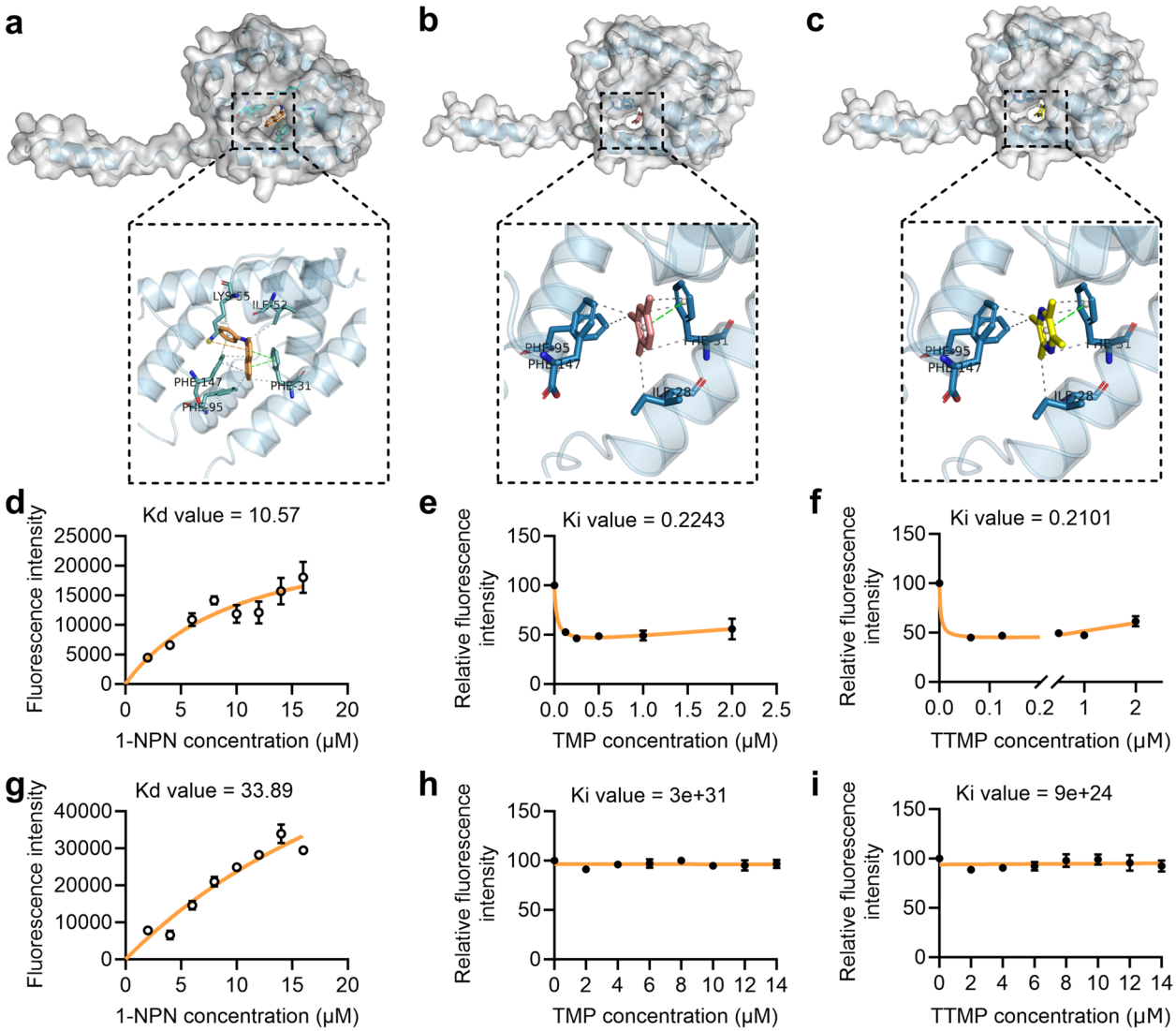

Fig. 3 Binding ability of Pbp5 to TMP and TTMP. **a** Binding sites prediction between Pbp5 and 1-NPN by Autodock Vina. **b** Binding sites prediction between Pbp5 and TMP by Autodock Vina. **c** Binding sites prediction between Pbp5 and TTMP by Autodock Vina. **d** Binding abilities of 1-NPN to Pbp5. **e** Competitive binding ability of TMP to 1-NPN and Pbp5 complex. **f** Competitive binding ability of TTMP to 1-NPN and Pbp5 complex. **g** Binding abilities of 1-NPN to Pbp5 mutant. **h** Competitive binding ability of TMP to 1-NPN and Pbp5 mutant complex. **i** Competitive binding ability of TTMP to 1-NPN and Pbp5 mutant complex

Obp99a peaked in the female head without antennae (Fig. 4c and d). Subsequent RNAi experiments resulted in a decrease of more than 50% in the expression levels of Pbp5 and Obp99a (Additional file 1: Fig. S3a and 3b), with no significant impact on survival observed (Additional file 1: Fig. S3c and 3d). Mating competition assays revealed that knocking down Pbp5 significantly reduced female mating number, whereas knocking down Obp99a had no effect on mating (Fig. 4e and f). Additionally, EAG responses to TMP, TTMP, and mixture of TMP and TTMP were significantly reduced in females with knocked down Pbp5 expression (Fig. 4g–i, Additional file 1: Fig. S4a–4c). These findings suggest that Pbp5 plays a role in female mating and response to sex pheromone-TMP and TTMP.

Tim affects the expression of Pbp5

Given that both Tim and Pbp5 are rhythmically expressed, we infer that Tim may influence expression of Pbp5. To test this hypothesis, we initially examined the tissue expression of Tim in female flies. The results revealed that Tim exhibited the highest expression in the antenna, similar to Pbp5 (Fig. 5a). Knocking down Tim through RNAi led to a decrease in Pbp5 expression

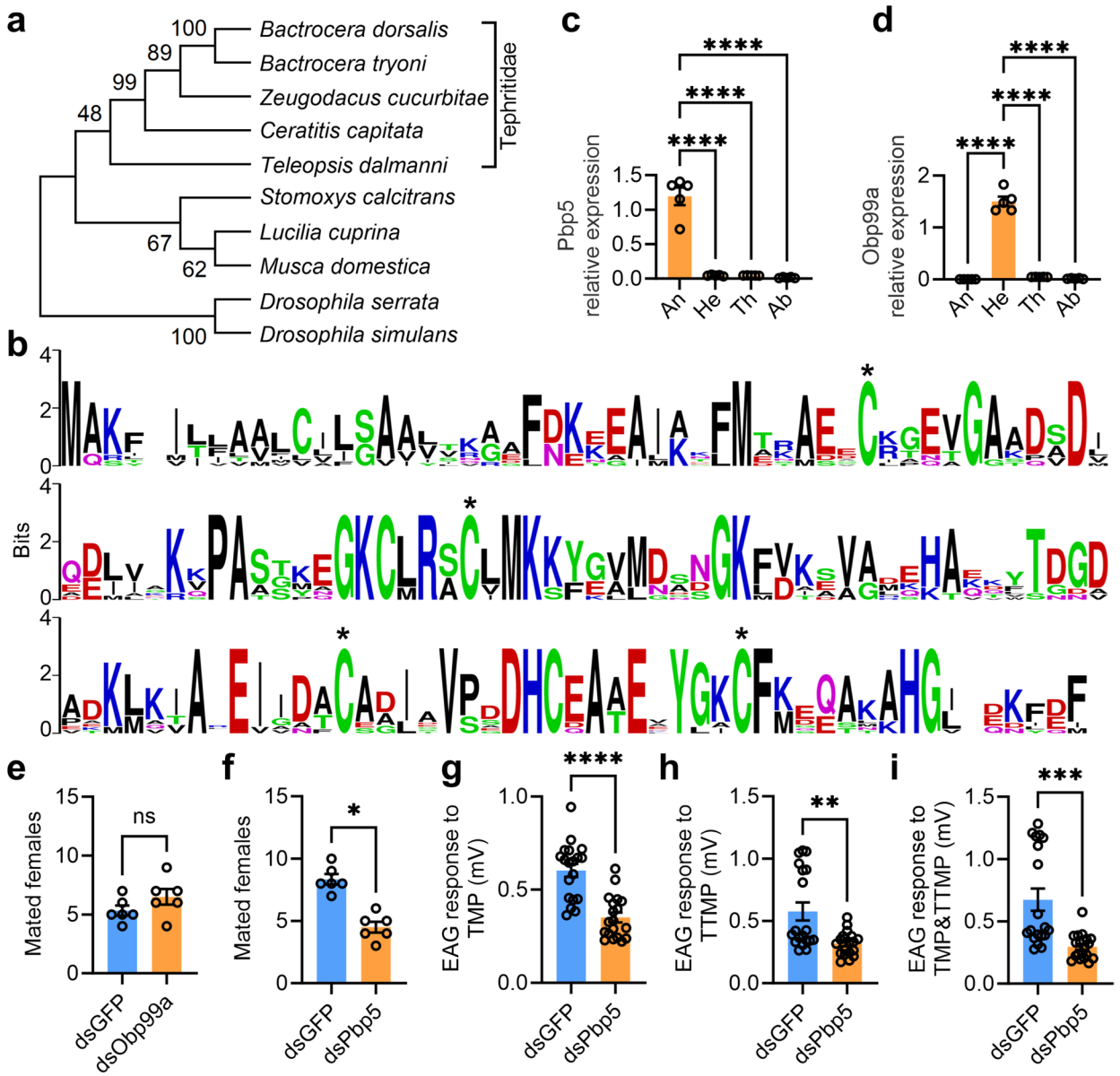

Fig. 4 RNAi of Pbp5 reduces female mating and EAG response to TMP and TTMP. **a** Maximum likelihood topology tree shows Pbp5 is conserved in Tephritidae. **b** Conservation of Pbp5 amino acids in Tephritidae. The image was generated using the complete amino acid sequences of the species in Tephritidae in **a**. **c** Female tissue expression of Pbp5 (replicates = 5, $F(3,16) = 82.79$, $P < 0.0001$, one-way ANOVA). **d** Female tissue expression of Obp99a (replicates = 5, $F(3,16) = 263.5$, $P < 0.0001$, one-way ANOVA). **e** Influence of Obp99a knockdown on female mating (replicates = 6, $P = 0.2722$, paired sample *t* test). **f** Influence of Pbp5 knockdown on female mating (replicates = 6, $P = 0.0047$, paired sample *t* test). **g** Influence of Pbp5 knockdown on female EAG response to TMP (replicates = 19, $P < 0.0001$, independent sample *t* test). **h** Influence of Pbp5 knockdown on female EAG response to TTMP (replicates = 19, $P = 0.0015$, independent sample *t* test). **i** Influence of Pbp5 knockdown on female EAG response to TMP and TTMP mixture (replicates = 19, $P = 0.0002$, independent sample *t* test)

(Fig. 5b and c). Additionally, knockdown of Tim significantly reduced female mating frequency (Fig. 5d) and EAG response to sex pheromone (Additional file 1: Fig. S5a–5c). To further confirm the relationship between Tim and Pbp5, we manipulated the circadian rhythm of female flies by subjecting them to darkness during daytime and light during nighttime. Subsequent gene expression analysis demonstrated a complete reversal in the patterns of Tim and Pbp5 expressions compared to normal reared flies (Fig. 2e and f), with both genes exhibiting peak expressions at 8:00 (Fig. 5e). Mating competition assays also indicated that fewer females with

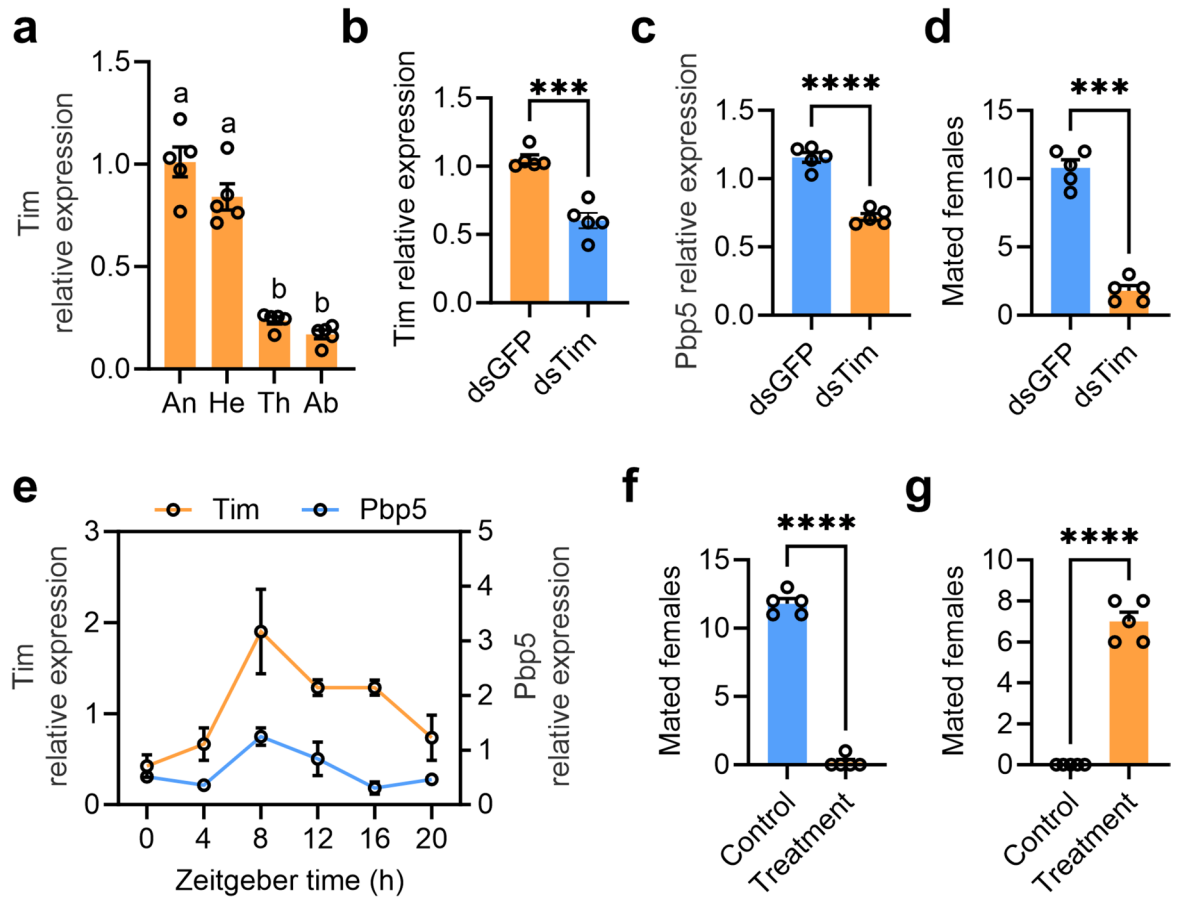

Fig. 5 Influence of Tim on Pbp5 expression and female mating. **a** Tissue expression pattern of Tim in females (replicates = 5, $F(3,16) = 70.45$, $P < 0.0001$, one-way ANOVA). **b** RNAi efficiency of Tim (replicates = 5, $P = 0.0001$, independent sample *t* test). **c** Relative expression of Pbp5 in female antenna after Tim knockdown (replicates = 5, $P < 0.0001$, independent sample *t* test). **d** Influence of Tim knockdown on mated female number (replicates = 5, $P = 0.0004$, paired sample *t* test). **e** Expression patterns of Tim and Pbp5 in the head and antenna of females with biological clock reversed (Tim: replicates = 4, $F(5,18) = 5.199$, $P = 0.004$, one-way ANOVA; Pbp5: replicates = 4, $F(5,18) = 4.954$, $P = 0.005$, one-way ANOVA). **f** Mated number of females with biological clock reversed in the evening (replicates = 5, $P < 0.0001$, paired sample *t* test). **g** Mated number of females with biological clock reversed in the morning (replicates = 5, $P < 0.0001$, paired sample *t* test)

reversed circadian rhythms mated with males than control females in the evening (20:00) (Fig. 5f), while more females with reversed circadian rhythms mated with males in the morning (8:00) (Fig. 5g). Consistently, EAG responses to sex pheromone decreased significantly for females with reversed circadian rhythms in the evening but increased significantly in the morning (Additional file 1: Fig. S5d–5i). These findings collectively suggest that Tim can affect both Pbp5 expression and female mating behavior.

Discussion

Studies have demonstrated the prevalence of TMP and TTMP as sex pheromones in certain Tephritidae species [22–24]. While the rectal *Bacillus* synthesis mechanisms of TMP and TTMP have been further elucidated [22], their olfactory recognition mechanisms remain unexplored. Our study has identified Pbp5 as an odorant binding protein that detects TMP and TTMP, thereby paving the way for further investigation into the olfactory recognition mechanism of these compounds. Given the common occurrence of TMP and TTMP in Tephritidae [22, 23], along with the high conservation of Pbp5 within this family, we hypothesize that the recognition mechanisms for these compounds may be shared among Tephritidae species. It is worth noting that Pbp5 is also present in other dipteran insects such as *Drosophila* [26]; however, studies have revealed that Pbp5 is not required for odorant transport in *Drosophila* [27]. Therefore, it cannot be ruled out that Pbp5 may also play additional roles in the olfactory process of *B. dorsalis*. Furthermore, the circadian influence on odorant receptors (Ors), which play a direct role in neuronal activation either independently or in conjunction with other factors such as

odorant binding proteins, may also impact the perception of sex pheromones. Although the Ors identified in the head transcriptome did not exhibit rhythmic expression, further research is needed to identify the specific Ors responsible for detecting sex pheromones.

It is notable that certain phenolic compounds, such as (*E*)-coniferyl alcohol (E-CF) and 2-allyl-4,5-dimethoxyphenol (DMP), are also considered to effectively enhance the male attraction to females and increase their mating success rate [28, 29]. Moreover, E-CF behaves in the same manner as TMP and TTMP, exerting a higher attraction to females at dusk [30]. However, both E-CF and DMP are derived from methyl eugenol (ME), which is a plant volatile [31]. E-CF and DMP can only be emitted after males ingest ME [32]. Nevertheless, in the natural and experimental populations, when males have no access to ME, they can still carry out mating behavior effectively, which might imply that these phenolic compounds can enhance the males' attraction to the females, but they are not indispensable.

Similar to other behaviors, olfactory perception plays a crucial role in guiding animal behavior, which can vary according to the time of day [33]. Recent research has demonstrated connections between the olfactory system and the biological clock [34, 35]. The expression of Obps and Ors, which are related to mating and foraging, may exhibit a strong correlation with circadian changes in environmental factors such as photoperiod and temperature [36, 37]. These environmental factors have the ability to modify olfactory recognition abilities. Our study also revealed that *B. dorsalis* detects sex pheromones (TMP and TTMP) in a circadian rhythm similar to beetles, *Drosophila*, and mosquitoes [36–40]. Furthermore, our research showed that Tim can influence the expression of Pbp5, thereby controlling females' sensitivity to sex pheromones and impacting their diurnal mating behavior. Tim is considered a core oscillatory gene in insect brains [41, 42]; mutant flies lacking Tim demonstrate an inability to respond to odors in a rhythmic manner, further confirming regulation by the circadian clock [43]. However, it is still unclear how Tim affects the expression of Pbp5, and the detailed regulatory pathway still needs to be further elucidated.

Our study still has certain limitations. While our behavioral and molecular experiments have confirmed that circadian mating behavior is influenced by changes in the rhythm of recognition ability to sex pheromone, we have only been able to identify the Obp responsible for sex pheromone in the olfactory system, with the related Ors remaining unknown. Additionally, while it has been demonstrated that Tim may indirectly affect the expression of Pbp5, the precise interaction mode between the rhythmic system and the olfactory system remains unclear.

Conclusions

In recent years, significant advancements have been achieved in the identification of the sex pheromone of male *B. dorsalis*. Specifically, it has been shown that rectal *Bacillus* of males utilizes glucose and amino acids as precursors to produce sex pheromone-TMP and TTMP [22–24]. However, there remains limited understanding regarding how females perceive TMP and TTMP released by males. This study demonstrates for the first time that odorant binding protein-Pbp5 is responsible for binding TMP and TTMP in female antennae. Furthermore, it has been revealed that the rhythmic mating behavior of females is associated with the rhythmic expression of Pbp5, which can be influenced by the clock gene-Tim. Our research significantly contributes to our comprehension of the rhythmic mating behavior exhibited by *B. dorsalis*.

Methods

Insect rearing

The *B. dorsalis* strain is reared under laboratory conditions (27 ± 1 °C, 12:12 h light:dark cycle, 70–80% RH). The larva is fed by a maize-based artificial diet containing 150 g of corn flour, 150 g of banana, 0.6 g of sodium benzoate, 30 g of yeast, 30 g of sucrose, 30 g of paper towel, 1.2 mL of hydrochloric acid and 300 mL of water. The adult is manually fed by solid diet (consisting of 50 g yeast hydrolysate and 50 g sucrose) and sterile water in daily.

Recording of female mating frequency at various time intervals throughout the day

To record the mating numbers of mature females (15 days old) at different times of day, 15 mature males and 15 mature females were placed in a 35 × 35 × 35 cm wooden cage. The day was divided into three observation periods (0:00–8:00, 8:00–16:00, 16:00–24:00), and the number of mated females during each period was recorded individually. Five replicate cages were observed for each time period.

Females attracted by sex pheromones at different time periods in a day

The attractiveness of sex pheromones (TMP and TTMP) to mature females was assessed at various time intervals throughout the day. Briefly, 100 ml of TMP and TTMP, diluted in ethanol (TMP: 2 mg/mL, TTMP: 1 mg/mL), were placed in traps made of transparent plastic vials (20 × 6 cm) sealed with a yellow lid featuring small entrances for fly entry. The attraction assay was conducted in a test chamber assembled with a ventilated lid-covered plastic cylinder (120 × 30 cm). The day was

divided into three observation periods (0:00–8:00, 8:00–16:00, 16:00–24:00), and the number of females trapped by the sex pheromone during each period was recorded separately. Eight replicates were recorded for each period.

EAG response recording

EAG analysis was conducted to assess the electrogram responses in the antenna of mature females exposed to TMP and TTMP. For EAG preparations, the antenna of a female was excised and positioned between two glass electrodes (with one electrode connected to the antenna tip). The antenna tip was gently trimmed to facilitate electrical contact. Diluted solutions of TMP and/or TTMP in ethanol were utilized as stimulants. Ten microliters of sex pheromone (TMP: 2 mg/mL, TTMP: 1 mg/mL) were applied onto the filter paper, which was then positioned near the air inlet and stimulated five times. The signals from the antennae were analyzed using GC-EAD 2014 software (version 4.6, Syntech). Solvent was used as a negative control to stimulate each tested antenna in the assays, and the resulting response values were recorded. Subsequently, the response values were obtained by stimulating the antennae with the compound dissolved in the solvent. Finally, for statistical analysis, we calculated the final result by subtracting the response value obtained from stimulating the antennae with the compound dissolved in solvent from that obtained by stimulating them with just solvent.

Transcriptome sequencing and gene identification

To identify the clock and olfactory genes that contribute to female mating preference, the female RNA-seq was done for mature female heads at different time periods in a day (0:00, 4:00, 8:00, 12:00, 16:00, 20:00). Five replicate samples were prepared for each period, with five heads dissected for RNA extraction per sample. Subsequently, paired-end RNA-seq libraries were prepared and sequenced on an Illumina HiSeq2000 platform. Briefly, raw reads were generated in FASTQ format and sorted by barcodes for further analysis. Prior to assembly, preprocessing of paired-end raw reads from each cDNA library was conducted to remove adapters, low-quality sequences ($Q < 20$), and reads contaminated with microbial sequences. Clean reads were then de novo assembled to produce contigs. An index of the reference genome of *B. dorsalis* was constructed, and paired-end clean reads were mapped to the reference genome using HISAT2 2.4 with parameters including "-rna-strandness RF" and defaults [44]. StringTie software was utilized to calculate normalized gene expression values (FPKM) for evaluating transcript expression abundances [45]. Subsequently, gene differential expression analysis was performed using DESeq2 software [46]. Genes/transcripts with a false discovery rate (FDR) below 0.01 and absolute fold change ≥ 2 were considered DEGs. Principal component analysis (PCA) was conducted using the R package gmodels to elucidate the structure/relationship of the samples. Pathway enrichment analysis was carried out to identify clock genes in the circadian rhythm pathway.

Expression validation of candidate genes by qRT-PCR

qRT-PCR analysis was used to validate gene expression in antenna and other tissues. Total RNA in the tissues of mature females was extracted using TRIzol reagent. Subsequently, cDNA synthesis was conducted utilizing the One-Step gDNA Removal and cDNA Synthesis SuperMix Kit (TransGen Biotech, Beijing, China). qRT-PCR was then performed using the PerfectStarTM Green qPCR SuperMix Kit (TransGen Biotech, Beijing, China) to assess gene expression levels. Gene-specific primers for the target genes were designed via primer blast on the NCBI website (Additional file 10: Table S2). Before conducting qPCR, the amplification efficiency of the primers was evaluated, and only primers with amplification efficiency within the range of 90–110% were used for further qPCR. The α-tubulin and actin genes were utilized as reference genes [47]. PCR procedures were conducted following the manufacturer's instructions. The three-step PCR procedures and melt curve analysis were carried out in accordance with the manufacturer's instructions. Specifically, the qPCR protocol included an initial denaturation at 95 ℃ for 30 s, followed by 40 cycles of PCR with denaturation at 95 ℃ for 5 s, annealing at 55℃ for 30 s, and extension at 72 ℃ for 30 s. The protocol concluded with a step to generate a melt curve, which involved an initial denaturation at 95 ℃ for 15 s, annealing at 60 ℃ for 30 s, and a final denaturation at 95 °C for another 15 s. Only experiments resulting in a single peak on the melt curve were considered as valid amplification reactions. Subsequently, data normalization was performed using the method of $2^{-\Delta\Delta Ct}$.

Phylogenetic sequence analysis

Phylogenetic analysis was conducted using amino acid sequence alignments for Obp sequences identified from insect genomes. Specifically, Pbp5 amino acid sequence was used to do protein-to-protein blast in NCBI. Then the top 10 most similar Obp sequences (accession number: XP_011198820.1, XP_039959984.1, XP_011193147.1, XP_004525016.1, XP_023303590.2, XP_037935942.1, XP_058983721.1, XP_013101515.1, XP_020809323.1, and XP_002078516.2) in other Diptera species were used to generate the phylogenetic tree. Obp amino acid sequence analyses were performed with MEGA11, and maximum likelihood (ML) tree reconstruction was performed using the Poisson model and

uniform rates [48]. The ML heuristic search was performed with the nearest neighbor-change method, and the initial tree was selected by applying the neighbor-joining method to a matrix of pairwise distances estimated using the JTT method. The accuracy of the tree was tested with bootstrapping using 100 replicates. The conservation of the Obp proteins was determined using the WebLogo tool (https://weblogo.berkeley.edu/logo.cgi).

RNA interference

Double-stranded RNA (dsRNA) primers, containing the T7 promoter sequence, were designed utilizing the coding sequences (CDSs) of the target genes as templates (Additional file 10: Table S2). The MEGAscript RNAi Kit (Thermo Fisher Scientific, USA) was employed for the synthesis and purification of dsRNA following the manufacturer's instructions. The GFP gene (GenBank accession number: AHE38523) served as the RNAi negative control. To induce a knockdown effect on the target genes, 0.5 μL dsRNA (1000 ng/μL) was injected into the abdomen. The knockdown efficiency of the genes was assessed using qRT-PCR 24h after dsRNA injection. Besides, the survival rate of 30 dsRNA-injected females was also recorded.

Mating competition assay

Mating competition assays between females with different treatments were conducted in a wooden cage (35 cm × 35 cm × 35 cm). Briefly, pronotum of females injected with dsRNA of Obp99a (Pbp5) and GFP were colored with different colors. Then 30 females injected dsRNA of Obp99a (Pbp5) and 30 females injected dsRNA of GFP were introduced into the wooden cage, in which 30 mature unmated males were placed. Then the mated female number was recorded during 20:00 to 22:00. Each assay was replicated five times.

For mating ability comparison between females with changed biological clocks and the controls, the same assays were done as the above methods.

Protein–ligand docking simulation

After homologous protein modeling was conducted using the Swiss-Model software, models with high scores were selected for subsequent model validation [49]. The quality of the Pbp5 model was assessed by Verify-3D, and ERRAT, within the SAVES V7.0 software [50]. TMP and TTMP models were downloaded from the NCBI website. Protein–ligand docking simulations were performed using Autodock Vina [51]. The binding result with the lowest binding energy was selected, processed using PyMOL [52], and further analyzed and visualized using ProteinPlus [53] and Protein–Ligand Interaction Profiler [54].

Binding ability of Pbp5 to TMP and TTMP

The recombinant Pbp5 protein was primarily obtained through in vitro expression in *Escherichia coli* Rosetta (DE3) cells, following a previously established protocol [55]. In brief, PCR primers with restriction sites were designed according to the CDS of Pbp5. Subsequently, PCR products were purified and ligated to the pet-sumo prokaryotic expression vector. The resulting vector was then transformed into *Escherichia coli* Rosetta (DE3) cells for expression. Positive clones were selected based on kanamycin resistance, and their sequences were confirmed through sequencing to ensure the correct sequence. Verified clones were cultured in LB medium supplemented with kanamycin at 37 ℃ for 16 h. Subsequently, 100 ml of bacterial culture was inoculated into an LB medium containing 0.1 mM IPTG and incubated at 18 ℃ for 8 h. The bacteria were then harvested by centrifugation at 8000 rpm and resuspended in lysis buffer (80 mM Tris–HCl, 200 mM NaCl, 1 mM EDTA, 4% glycerol, pH 7.2, 0.5 mM PMSF). Sonication (3 s, five passes) was performed to lyse the bacterial cells. The recombinant proteins present in the supernatant were collected by centrifugation. Subsequently, the proteins were purified by two rounds of anion-exchange chromatography and concentrated using an ultrafiltration cube. The purity of the purified recombinant proteins was confirmed by SDS-PAGE analysis. Another recombinant protein Pbp5-mutant, whose binding sites for TMP and TTMP were mutated, was also prepared with the method above. Specifically, according to the docking results, the binding sites (Ile-28, Phe-31, Phe-95, and Phe-147) (Additional file 10: Table S1) of Pbp5 were mutated to alanine.

Then the fluorescence binding assay using 1-NPN with Pbp was conducted on a Microplate Reader (ThermoScientific Varioskan LUX), following a method previously described in locust studies [56]. The excitation wavelength was set at 337 nm, and the emission wavelength was set at 380–520 nm. Pbp5 or Pbp5-mutant (2 μM dissolved in 50 mM Tris–HCl, pH = 7.4) was mixed with 1-NPN (2 μM-16 μM dissolved in chromatographic methanol), and the maximum fluorescence intensity was recorded. A nonlinear regression analysis for one-site-specific binding was carried out based on the gradient fluorescence intensity. The dissociation constant (Kd) and the maximum fluorescence intensity (Bmax) for the binding of 1-NPN to the protein were computed.

For competitive binding assays, various concentrations of TMP or TTMP (dissolved in chromatographic methanol) were incrementally added to the mixture of the recombinant protein and 1-NPN (2 μM dissolved in 50

mM Tris–HCl, pH = 7.4). Subsequently, the fluorescence intensity at different concentrations of TMP or TTMP was recorded. The inhibition constant (Ki) for TMP or TTMP competing with 1-NPN was calculated based on the fluorescence intensity. A lower Ki value indicates a stronger affinity between the protein and TMP or TTMP.

Data analysis

Statistical analysis methods used in the study were indicated in the figure legends. Differences were considered significant when $P < 0.05$. All data were analyzed using the GraphPad Prism version 10, GraphPad Software, La Jolla, CA, USA, https://www.graphpad.com/

Abbreviations

TMP	Trimethylpyrazine
TTMP	Tetramethylpyrazine
EAG	Electroantennogram
Tim	Timeless
DEGs	Differentially expressed genes
Csps	Chemosensory proteins
Obps	Odorant binding proteins
Ors	Odorant receptors
Pbp5	Pheromone binding protein 5
Obp99a	Odorant binding protein 99a
1-NPN	*N*-Phenyl-1-naphthylamine
Kd	Dissociation constant
Ki	Inhibition constant
E-CF	(E)-coniferyl alcohol
DMP	2-Allyl-4,5-dimethoxyphenol
ME	Methyl eugenol

Supplementary Information

The online version contains supplementary material available at https://doi.org/10.1186/s12915-025-02164-4.

Additional file 1. Fig. S1. Difference of head transcriptome at different time of a day

Additional file 2. Fig. S2. RNAi of Pbp5 and Obp99a

Additional file 3. Fig. S3. Example traces of Pbp5 knocked down female antenna responses to sex pheromone

Additional file 4. Fig. S4. Construction and evaluation of Pbp5 protein model

Additional file 5. Influence of Tim and biological rhythm on female EAG response to sex pheromone

Additional file 6. Dataset S1. Head gene expression profile. Dataset S2. DE genes screening between head at 20:00 and 0:00

Additional file 7. Dataset S3 DE genes screening between head at 20:00 and 4:00. Dataset S4 DE genes screening between head at 20:00 and 8:00

Additional file 8. Dataset S5 DE genes screening between head at 20:00 and 12:00. Dataset S6 DE genes screening between head at 20:00 and 16:00

Additional file 9. Dataset S7 Expression of DEG in Circadian rhythm pathway. Dataset S8 Expression of olfactory genes

Additional file 10. Tables S1-S2. Table S1 Predication of binding site amino acid residue of Pbp5. Table S2 Primers used in the study

Acknowledgements

We thank Guangzhou Genedenovo Biotechnology Co., Ltd., for assisting in sequencing.

Authors' contributions

D.C. and Y.J. conceived and designed the project. Y.J. and G.L. performed experiments and analyzed data. D.C. made the graphs. D.C. and Y.J. wrote the manuscript. D.C. and Y.L. provided the research platform. All authors read and approved the final manuscript.

Funding

The study was funded by the National Natural Science Foundation of China (No. 32372520 and No. 3212200346) and the National Key Research and Development Program of China (No. 2023YFD1401401-08).

Data availability

All the data needed to evaluate the conclusions in the paper are presented in the paper and/or the Supplementary Materials. The accession number of Tim, Pbp5 and Obp99a are XM_011215785.4, XM_011200518.4 and XM_011206554.3, respectively. RNA-sequencing data have been deposited in the Genome Sequence Read Archive Database of the National Genomics Data Center (CRA022721).

Declarations

Ethics approval and consent to participate

Not applicable.

Consent for publication

Not applicable.

Competing interests

The authors declare no competing interests.

Received: 19 August 2024 Accepted: 17 February 2025
Published online: 23 February 2025

References

1. Wade MJ. The evolution of insect mating systems. Evolution. 1984;38(3):706–8.
2. Evans HE. Insect behavior. Science. 1976;194(4265):612–3.
3. Dixson A. Mating systems and strategies. Am J Hum Biol. 2005;17(3):390–1.
4. Slessor KN, Winston ML, Le Conte Y. Pheromone communication in the honeybee (Apis mellifera L.). J Chem Ecol. 2005;31(11):2731–45.
5. Woods WA Jr, Hendrickson H, Mason J, Lewis SM. Energy and predation costs of firefly courtship signals. Am Nat. 2007;170(5):702–8.
6. Wagner WE Jr, Reiser MG. The importance of calling song and courtship song in female mate choice in the variable field cricket. Anim Behav. 2000;59(6):1219–26.
7. Spieth HT. Courtship behavior in *Drosophila*. Annu Rev Entomol. 1974;19:385–405.
8. Saunders DS. The biological clock of insects. Sci Am. 1976;234(2):114–21.
9. Soma M. Behavioral and evolutionary perspectives on visual lateralization in mating birds: a short systematic review. Front Physiol. 2022;12:12.
10. Chen S, Zhou Y, Chen Y, Gu J. fastp: an ultra-fast all-in-one FASTQ preprocessor. Bioinformatics. 2018;34(17):884–90.
11. Zhang SL, Yue Z, Arnold DM, Artiushin G, Sehgal A. A circadian clock in the blood-brain barrier regulates xenobiotic efflux. Cell. 2018;173(1):130-+.
12. Ito C, Tomioka K. Heterogeneity of the peripheral circadian systems in *Drosophila melanogaster*: a review. Front Physiol. 2016;7:8.
13. Yao Z, Shafer OT. The *Drosophila* circadian clock is a variably coupled network of multiple peptidergic units. Science. 2014;343(6178):1516–20.
14. Mazuski C, Abel JH, Chen SP, Hermanstyne TO, Jones JR, Simon T, et al. Entrainment of circadian rhythms depends on firing rates and neuropeptide release of VIP SCN neurons. Neuron. 2018;99(3):555-+.
15. Mohawk JA, Green CB, Takahashi JS. Central and peripheral circadian clocks in mammals. In: Hyman SE, editor. Annu Rev Neurosci. 2012;35:445–62.

16. Tomioka K, Matsumoto A. A comparative view of insect circadian clock systems. Cell Mol Life Sci. 2010;67(9):1397–406.
17. Miyamoto T, Amrein H. Suppression of male courtship by a *Drosophila* pheromone receptor. Nat Neurosci. 2008;11(8):874–6.
18. Clowney EJ, Iguchi S, Bussell JJ, Scheer E, Ruta V. Multimodal chemosensory circuits controlling male courtship in *Drosophila*. Neuron. 2015;87(5):1036–49.
19. Wada-Katsumata A, Schal C. Antennal grooming facilitates courtship performance in a group-living insect, the German cockroach Blattella germanica. Sci Rep. 2019;9:9.
20. Pittendrigh CS. Temporal organization: reflections of a Darwinian clock-watcher. Annu Rev Physiol. 1993;55:16–54.
21. Vaz Nunes M, Saunders D. Photoperiodic time measurement in insects: a review of clock models. J Biol Rhythms. 1999;14(2):84–104.
22. Ren L, Ma Y, Xie M, Lu Y, Cheng D. Rectal bacteria produce sex pheromones in the male oriental fruit fly. Curr Biol. 2021;31(10):2220-+.
23. Gao Z, Xie M, Gui S, He M, Lu Y, Wang L, et al. Differences in rectal amino acid levels determine bacteria-originated sex pheromone specificity in two closely related flies. ISME J. 2023;17(10):1741–50.
24. Gui SY, Yuval B, Engl T, Lu YY, Cheng DF. Protein feeding mediates sex pheromone biosynthesis in an insect. eLife. 2023;12:e83469.
25. Ha TS, Smith DP. Recent insights into insect olfactory receptors and odorant-binding proteins. Insects. 2022;13(10):926.
26. Anholt RRH, Williams TI. The soluble proteome of the *Drosophila* Antenna. Chem Senses. 2010;35(1):21–30.
27. Larter NK, Sun JS, Carlson JR. Organization and function of *Drosophila* odorant binding proteins. eLife. 2016;5:e20242.
28. Khoo CCH, Tan KH. Rectal gland of Bactrocera papayae: ultrastructure, anatomy, and sequestration of autofluorescent compounds upon methyl eugenol consumption by the male fruit fly. Microsc Res Tech. 2005;67(5):219–26.
29. Deng SZ, Li XY, Wang ZM, Wang JB, Han DY, Fan JH, et al. Assessment of 2-allyl-4,5-dimethoxyphenol safety and attractiveness to mature males of Bactrocera dorsalis (Hendel). Ecotoxicol Environ Saf. 2021;223:112567.
30. Liu H, Wang D-D, Wan L, Hu Z-Y, He T-T, Wang J-B, et al. Assessment of attractancy and safeness of (Econiferyl alcohol for management of female adults of Oriental fruit fly, Bactrocera dorsalis (Hendel). Pest Manag Sci. 2022;78(3):1018–28.
31. Raghu S, Clarke AR. Spatial and temporal partitioning of behaviour by adult dacines: direct evidence for methyl eugenol as a mate rendezvous cue for Bactrocera cacuminata. Physiol Entomol. 2003;28(3):175–84.
32. Tan KH, Tokushima I, Ono H, Nishida R. Comparison of phenylpropanoid volatiles in male rectal pheromone gland after methyl eugenol consumption, and molecular phylogenetic relationship of four global pest fruit fly species: Bactrocera invadens, B. dorsalis, B. correcta and B. zonata. Chemoecology. 2011;21(1):25–33.
33. Gadenne C, Barrozo RB, Anton S. Plasticity in insect olfaction: to smell or not to smell? In: Berenbaum MR, editor. Annu Rev Entomol. 2016;61:317–33.
34. Page TL, Koelling E. Circadian rhythm in olfactory response in the antennae controlled by the optic lobe in the cockroach. J Insect Physiol. 2003;49(7):697–707.
35. Decker S, McConnaughey S, Page TL. Circadian regulation of insect olfactory learning. Proc Natl Acad Sci U S A. 2007;104(40):15905–10.
36. Wang Y, Dong H, Qu Y, Zhou Y, Qin J, Li K, et al. Circabidian rhythm of sex pheromone reception in a scarab beetle. Curr Biol. 2024;34(3):568.
37. Siciliano P, Scolari F, Gomulski LM, Falchetto M, Manni M, Gabrieli P, et al. Sniffing out chemosensory genes from the Mediterranean fruit fly, *Ceratitis capitata*. PLoS One. 2014;9(1):e85523.
38. Das S, Dimopoulos G. Molecular analysis of light pulse stimulated blood feeding inhibition in Anopheles gambiae. Am J Trop Med Hyg. 2008;79(6):333-.
39. Wang G, Vega-Rodriguez J, Diabate A, Liu J, Cui C, Nignan C, et al. Clock genes and environmental cues coordinate Anopheles pheromone synthesis, swarming, and mating. Science. 2021;371(6527):411-+.
40. Tanoue S, Krishnan P, Krishnan B, Dryer SE, Hardin PE. Circadian clocks in antennal neurons are necessary and sufficient for olfaction rhythms in *Drosophila*. Curr Biol. 2004;14(8):638–49.
41. Shafer OT, Gutierrez GJ, Li K, Mildenhall A, Spira D, Marty J, et al. Connectomic analysis of the *Drosophila* lateral neuron clock cells reveals the synaptic basis of functional pacemaker classes. eLife. 2022;11:e79139.
42. Ma D, Ojha P, Yu AD, Araujo MS, Luo W, Keefer E, et al. Timeless noncoding DNA contains cell-type preferential enhancers important for proper Drosophila circadian regulation. Proc Natl Acad Sci U S A. 2024;121(15):e2321338121-e.
43. Krishnan B, Dryer SE, Hardin PE. Circadian rhythms in olfactory responses of Drosophila melanogaster. Nature. 1999;400(6742):375–8.
44. Kim D, Langmead B, Salzberg SL. HISAT: a fast spliced aligner with low memory requirements. Nat Methods. 2015;12(4):357-U121.
45. Pertea M, Pertea GM, Antonescu CM, Chang T-C, Mendell JT, Salzberg SL. StringTie enables improved reconstruction of a transcriptome from RNA-seq reads. Nat Biotechnology. 2015;33(3):290-+.
46. Love MI, Huber W, Anders S. Moderated estimation of fold change and dispersion for RNA-seq data with DESeq2. Genome Biol. 2014;15(12):550.
47. Shen GM, Jiang HB, Wang XN, Wang JJ. Evaluation of endogenous references for gene expression profiling in different tissues of the oriental fruit fly Bactrocera dorsalis (Diptera: Tephritidae). BMC Molecular Biology. 2010;11:76.
48. Tamura K, Stecher G, Kumar S. MEGA11 molecular evolutionary genetics analysis version 11. Mol Biol Evol. 2021;38(7):3022–7.
49. Biasini M, Bienert S, Waterhouse A, Arnold K, Studer G, Schmidt T, et al. SWISS-MODEL: modelling protein tertiary and quaternary structure using evolutionary information. Nucleic Acids Res. 2014;42(Web Server issue):W252-8.
50. Laskowski RA, Rullmannn JA, MacArthur MW, Kaptein R, Thornton JM. AQUA and PROCHECK-NMR: programs for checking the quality of protein structures solved by NMR. J Biomol NMR. 1996;8(4):477–86.
51. Eberhardt J, Santos-Martins D, Tillack AF, Forli S. AutoDock Vina 1.2.0: new docking methods, expanded force field, and python bindings. J Chem Inf Model. 2021;61(8):3891–8.
52. Grell L, Parkin C, Slatest L, Craig PA. Viz, a tool for simplifying molecular viewing in PyMOL. Biochem Mol Biol Educ. 2006;34(6):402–7.
53. Schoening-Stierand K, Diedrich K, Faehrrolfes R, Flachsenberg F, Meyder A, Nittinger E, et al. Proteins plus: interactive analysis of protein-ligand binding interfaces. Nucleic Acids Res. 2020;48(W1):W48–53.
54. Salentin S, Schreiber S, Haupt VJ, Adasme MF, Schroeder M. PLIP: fully automated protein-ligand interaction profiler. Nucleic Acids Res. 2015;43(W1):W443–7.
55. Tian Z, Qiu G, Li Y, Zhang H, Yan W, Yue Q, et al. Molecular characterization and functional analysis of pheromone binding proteins and general odorant binding proteins from *Carposina sasakii* Matsumura (Lepidoptera: Carposinidae). Pest Manag Sci. 2019;75(1):234–45.
56. Ban L, Scaloni A, D'Ambrosio C, Zhang L, Yan Y, Pelosi P. Biochemical characterization and bacterial expression of an odorant-binding protein from *Locusta migratoria*. Cell Mol Life Sci. 2003;60(2):390–400.

Publisher's Note